BJ www.biochemj.org

BJ Structure

Biochem. J. (2009) **421**, 243–251 (Printed in Great Britain) doi:10.1042/BJ20090427

NEMO oligomerization and its ubiquitin-binding properties

Frank J. IVINS[1], Mark G. MONTGOMERY[1,2], Susan J. M. SMITH, Aylin C. MORRIS-DAVIES, Ian A. TAYLOR and Katrin RITTINGER[3]

Division of Molecular Structure, MRC-National Institute for Medical Research, The Ridgeway, London NW7 1AA, U.K.

The IKK [IκB (inhibitory κB) kinase] complex is a key regulatory component of NF-κB (nuclear factor κB) activation and is responsible for mediating the degradation of IκB, thereby allowing nuclear translocation of NF-κB and transcription of target genes. NEMO (NF-κB essential modulator), the regulatory subunit of the IKK complex, plays a pivotal role in this process by integrating upstream signals, in particular the recognition of polyubiquitin chains, and relaying these to the activation of IKKα and IKKβ, the catalytic subunits of the IKK complex. The oligomeric state of NEMO is controversial and the mechanism by which it regulates activation of the IKK complex is poorly understood. Using a combination of hydrodynamic techniques we now show that apo-NEMO is a highly elongated, dimeric protein that is in weak equilibrium with a tetrameric assembly. Interaction with peptides derived from IKKβ disrupts formation of the tetrameric NEMO complex, indicating that interaction with IKKα and IKKβ and tetramerization are mutually exclusive. Furthermore, we show that NEMO binds to linear di-ubiquitin with a stoichiometry of one molecule of di-ubiquitin per NEMO dimer. This stoichiometry is preserved in a construct comprising the second coiled-coil region and the leucine zipper and in one that essentially spans the full-length protein. However, our data show that at high di-ubiquitin concentrations a second weaker binding site becomes apparent, implying that two different NEMO–di-ubiquitin complexes are formed during the IKK activation process. We propose that the role of these two complexes is to provide a threshold for activation, thereby ensuring sufficient specificity during NF-κB signalling.

Key words: analytical ultracentrifugation (AUC), IKK (inhibitory κB kinase) complex, isothermal titration calorimetry (ITC), multi-angle light scattering (MALS), protein–protein interaction, ubiquitin.

INTRODUCTION

NF-κB (nuclear factor κB) transcription factors are key regulators of immune and inflammatory responses (reviewed in [1,2]). In unstimulated cells they are found in complex with IκB (inhibitory κB) proteins, an interaction that prevents their translocation to the nucleus and retains NF-κBs in the cytosol. Stimulus-dependent phosphorylation of IκBs induces their Lys^{48}-linked ubiquitination and subsequent degradation by the 26S proteasome, thereby liberating NF-κB and allowing nuclear translocation. A key regulator of this process is the multi-subunit IKK (IκB kinase) complex (sometimes referred to as the signalosome), which is composed of two kinases, IKKα and IKKβ, and a non-catalytic regulatory subunit called IKKγ or NEMO (NF-κB essential modulator) [3–5]. The apparent molecular mass of the resting IKK complex has been shown to be in the 700–900 kDa range, suggesting that it may contain multiple copies of its constituents [6–8]. Nonetheless, its precise composition is controversial, and it may be that its size varies in a stimulus-dependent manner [9]. NEMO is the regulatory hub of the IKK complex and integrates multiple signals, including phosphorylation, ubiquitination and interaction with ubiquitin chains [10]. In addition to being the target of multiple post-translational modifications, NEMO also acts as an assembly platform that facilitates the incorporation of a variety of proteins into the IKK signalosome, such as the viral proteins vFLIP {viral FLICE [FADD (Fas-associated death domain)-like interleukin 1β-converting enzyme]-inhibitory protein} and Tax, which can act as potent activators of NF-κB [11,12].

NEMO is a ~50 kDa protein predicted to consist of two coiled-coil regions, CC1 and CC2, a LZ (leucine zipper) and a ZF (zinc finger) (Figure 1). In spite of extensive studies aimed at defining the assembly of NEMO, its oligomeric state still remains a matter of some controversy. The apo form of the full-length protein has variously been described as monomeric, dimeric, trimeric or tetrameric state [13–15]. A number of studies have suggested that the second coiled-coil region, together with the LZ, constitutes the minimal oligomerization domain (from now on referred to as CoZi) [15,16]. However, similar to the full-length protein, the oligomeric state of this region is not clear and has, for example, been described as a trimer that can associate to 'pseudo-hexamers' upon appropriate stimulation [16]. In contrast, two recent crystal structures of this region have shown it forms a parallel, dimeric coiled-coil, in accordance with other studies that reported a dimeric assembly [15,17–19]. The oligomeric state of the N-terminal coiled-coil region is similarly unresolved, and a range of oligomeric states have been reported [20–22].

A key step towards a better understanding of the regulatory role of NEMO in NF-κB activation was the observation that NEMO interacts specifically with polyubiquitin chains ([23], but see [23a], [24]). These experiments initially utilized linear ('genetically linked', i.e. Gly^{76} to Met^{1} linked) polyubiquitin chains in a yeast two-hybrid screen. However, Lys^{63}-linked ubiquitin chains attached to RIP1 (receptor interaction protein kinase) are believed to be the physiological targets ([23], but see [23a]). This interaction is suggested to recruit the IKK complex to receptor complexes and thereby promote the subsequent

Abbreviations used: AUC, analytical ultracentrifugation; CoZi, C-terminal portion of NEMO encompassing the second coiled-coil region and the leucine zipper domain; IκB, inhibitory κB; IKK, IκB kinase; IKK_{NBD}, IKKβ NEMO-binding domain; ITC, isothermal titration calorimetry; LZ, leucine zipper; MALS, multi-angle laser light scattering; NF-κB, nuclear factor κB; NEMO, NF-κB essential modulator; $NEMO_{355}$, NEMO residues 1–355, with mutations C54S and K285N; SEC, size-exclusion chromatography; TCEP, tris-(2-carboxyethyl)phosphine; RI, refractive index; RIP1, receptor interaction protein kinase; vFLIP, viral FLICE [FADD (Fas-associated death domain)-like interleukin 1β-converting enzyme]-inhibitory protein; ZF, zinc finger.

[1] These authors contributed equally to this work.

[2] Present address: UCL Medical School – Royal Free Campus, Rowland Hill Street, London NW3 2PF, U.K.

[3] To whom correspondence should be addressed (email katrin.rittinger@nimr.mrc.ac.uk).

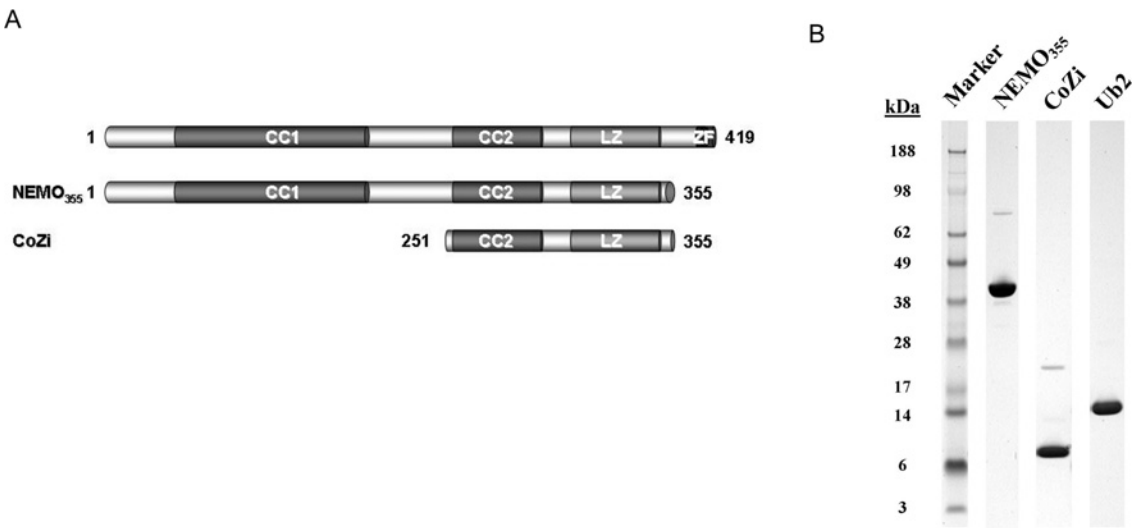

Figure 1 Structure and purity of protein constructs used in the present study

(**A**) Schematic representation of the domain structure of NEMO and the constructs used in the present study. (**B**) Coomassie Blue-stained SDS/polyacrylamide gel showing the purity of the protein preparations used. The faint bands on the $NEMO_{355}$ and CoZi lanes at twice the molecular mass represent incompletely denatured dimers. Molecular masses are shown to the left in kDa.

activation of the kinase activity of IKKα and IKKβ. The binding site for ubiquitin has been mapped to a region of NEMO that has homology with ABIN (A20-binding inhibitor of NF-κB) and optineurin and has been named the NUB or UBAN motif ([23], but see [23a], [24,25]). This conserved binding region is located within the CoZi domain. Although a number of studies have shown that specific recognition of K63-linked ubiquitin chains is important for NF-κB activation ([23], but see [23a], [24]), it has recently been reported that linear di-ubiquitin binds with a 100-fold higher affinity to the CoZi domain than K63-linked di-ubiquitin [17,18,26]. This observation is particularly interesting in the light of a recent report that NEMO itself becomes modified with linear ubiquitin chains that are attached by the ligase complex LUBAC [27].

In the present study we have applied a combination of complementary hydrodynamic methods to define the oligomeric state of NEMO and resolve the current controversy surrounding its self-association. We show that apo-NEMO forms a tight dimer that is in a relatively weak equilibrium with a tetrameric assembly. Importantly, binding of IKKβ-derived peptides prevented formation of the tetramer, indicating that the IKK-binding region in the N-terminal portion of NEMO is responsible for the formation of higher-molecular-mass species and that IKK binding and tetramerization are mutually exclusive. Furthermore, we show that the CoZi domain and a nearly full-length NEMO construct bind di-ubiquitin with similar affinities but slightly different energetics. These results suggest that no major conformational changes take place upon interaction with ubiquitin chains, but that minor rearrangements may be induced in the N-terminal coiled-coil region. Surprisingly, only one di-ubiquitin chain binds to the symmetrical NEMO dimer. However, a second binding site becomes apparent at high ubiquitin concentrations, implying that two different NEMO/polyubiquitin complexes are formed during the activation process. This observation may have implications for the *in vivo* function of NEMO and suggests that association with protein assemblies that provide a high density of poly-ubiquitin chains might induce clustering of NEMO, which in turn will lead to activation of the IKK complex.

EXPERIMENTAL

Plasmids

The cDNA for full-length mouse and human NEMO and the expression plasmid for di-ubiquitin were kindly provided by Dr F. Randow (MRC-LMB, Cambridge, U.K.). NEMO residues 251–355 (CoZi), NEMO (residues 1–355, C54S, K285N referred to as $NEMO_{355}$) and human NEMO residues 218–363 were cloned into the pGEX-6P1 expression vector. The C54S mutation was introduced to prevent disulfide bond formation, K285N has been described in [19]. Bovine mono-ubiquitin was purchased from Sigma.

Protein purification

For CoZi purification, *Escherichia coli* BL21(DE3) cells containing the plasmid were grown in LB (Luria–Bertani) broth at 37 °C to a D_{600} of ~0.8. Protein expression was induced by the addition of 0.5 mM IPTG (isopropyl β-D-thiogalactoside) and cells were incubated for a further 3 h. Cell pellets were resuspended in Buffer A {50 mM Tris/HCl, pH 8, 500 mM NaCl and 0.5 mM TCEP [tris-(2-carboxyethyl)phosphine]}, lysed by sonication and the crude lysate was applied to a pre-equilibrated glutathione–Sepharose column (GE Healthcare) at 1 ml/min. Bound protein was eluted with Buffer A containing 20 mM reduced glutathione. The GST affinity tag was removed by the addition of 3C protease and incubation at 4 °C overnight. The sample was concentrated in 10-kDa-molecular-mass-cut-off Vivaspin concentrators (Sartorius) and applied to a Superdex 75 column (GE Healthcare) pre-equilibrated with Buffer B (50 mM Tris/HCl, pH 8, 100 mM NaCl and 0.5 mM TCEP). Fractions containing CoZi were pooled and loaded on to another GSH column to remove contaminating GST and 3C protease. CoZi was concentrated to 20 mg/ml.

For $NEMO_{355}$ purification, expression was carried out in Rosetta2(DE3)pLysS cells at 18 °C for 16 h. Cell pellets were resuspended in $Buffer^{GST}$ (20 mM Tris/HCl, pH 8, 500 mM NaCl, 10 % glycerol and 0.25 mM TCEP) and lysed by sonication.

Crude lysate was applied to a column of glutathione–Sepharose resin followed by extensive washing with Buffer^{GST}. The GST affinity tag was removed on-column by overnight incubation with 1.5 mg of 3C protease. GST-free $NEMO_{355}$ was eluted in Buffer^{Q} (20 mM Tris/HCl, pH 8, 50 mM NaCl, 10 % glycerol and 0.25 mM TCEP) and applied to a Source Q ion-exchange column (GE Healthcare). The sample was eluted with a 1 M NaCl 20 column volume gradient in Buffer^{Q}, and concentrated to 5 ml on a 50-kDa-molecular-mass-cut-off Vivaspin concentrator. The sample was then applied to a Superdex 200 size-exclusion column pre-equilibrated in Buffer^{GST}. The relevant fractions were concentrated to 13.7 mg/ml.

For linear di-ubiquitin purification, expression was carried out in BL21(DE3) cells for 3 h at 37 °C. Purification was carried out as described previously for CoZi, except that the affinity tag was removed by incubation with TEV protease instead of 3C protease. Pure protein was concentrated using-5-kDa-molecular-mass-cut-off Vivaspin columns to 13.3 mg/ml.

Protein concentrations were determined by UV spectrometry using calculated 280 nm molar absorption coefficients. Concentrations were confirmed by analysis of the differential RI (refractive index) eluate peaks from the SEC (size-exclusion chromatography)-MALS (multi-angle light scattering) experiments described below. Specifically, integration of an RI peak yields a total mass that, in conjunction with known loading volume, allows determination of the loading concentration independent of UV absorbance. Concentration values from both methods were in good agreement. Furthermore, expected formula molecular masses were confirmed for each protein using MS.

ITC (isothermal titration calorimetry)

All samples were extensively dialysed into fresh buffer [50 mM Tris/HCl, pH 8, 0.5 mM TCEP and 100 mM NaCl (CoZi) or 150 mM NaCl ($NEMO_{355}$)]. Protein concentration was determined by UV absorbance and confirmed by the integration of RI peaks from SEC-MALS (see below). ITC measurements were carried out at 10 °C, 18 °C and 25 °C on a VP-ITC or ITC200 MicroCalorimeter (MicroCal Inc). In most cases, ITC titrations were carried out with 29 consecutive 10 μl injections of ubiquitin into the cell containing NEMO on the VP-ITC or alternatively with 19 consecutive 2 μl injections on the ITC200 instrument (all at various concentrations). ITC data were analysed with Origin7 software (MicroCal) supplied by the manufacturer. The heat capacity change was determined from the slope of a linear regression fit of ΔH plotted against the temperature of the titration.

MALS

Molecular mass and molecular-mass distributions were determined using on-line SEC-MALS. Samples were applied in a volume of 100 μl to a Superdex 200 10/300 GL column equilibrated in 20 mM Tris/HCl, 150 mM NaCl and 0.25 mM TCEP, pH 8.0, at a flow rate of 0.5 ml/min. The column was mounted on a Jasco HPLC controlled by the Chrompass software package. The scattered light intensity of the column eluate was recorded at 16 angles using a DAWN-HELEOS laser photometer (Wyatt Technology, Santa Barbara, CA, U.S.A.). The protein concentration of the eluent was determined from the RI(n) change ($dn/dc = 0.186$) (where c is solute concentration) using an OPTILAB-rEX differential refractometer equipped with a Peltier temperature-regulated flow cell, maintained at 25 °C (Wyatt Technology). The wavelength of the laser in the DAWNHELEOS and the light source in the OPTILABrEX was 658 nm. The weight-averaged molecular mass of material contained in chromatographic peaks was determined using the ASTRA software version 5.1 (Wyatt Technology Corp., Santa Barbara, CA). Briefly, at 1 s intervals throughout the elution of peaks, the scattered-light intensities, together with the corresponding protein concentrations, were used to construct Debye plots [KC/R_θ against $\sin^2(\theta/2)$]. The weight-averaged molecular mass was then calculated at each point in the chromatogram from the intercept of an individual plot. An overall average molecular mass and polydispersity term for each species was calculated by combining and averaging the results from the individual measurements.

Sedimentation-velocity AUC (analytical ultracentrifugation)

Sedimentation-velocity experiments were performed in a Beckman Optima Xli analytical ultracentrifuge, using conventional charcoal-filled Epon double-sector quartz cells or aluminium double-sector sapphire cells in an An-50 Ti rotor. The rotor speed was 40 000 rev./min or 50 000 rev./min respectively, and the temperature was maintained at 293 K. Prior to centrifugation, protein samples were dialysed exhaustively against the buffer blank (10 mM Tris/HCl, pH 8.0, 150 mM NaCl and 0.25 mM TCEP). The protein concentration was varied from 0.37 mg/ml to 1.76 mg/ml. Interference images were collected every 180 s during the sedimentation run. The data recorded from moving boundaries were analysed by the program SEDFIT in terms of both discrete species and continuous distribution function of sedimentation coefficient [$c(s)$].

RESULTS

$NEMO_{355}$ exists in a dimer/tetramer equilibrium

In order to resolve the discrepancies concerning the exact multimeric state of NEMO, the solution molecular mass of a construct containing all of the predicted coiled-coil regions was examined by SEC coupled to MALS (SEC-MALS). This construct is missing only the C-terminal ZF, which has been shown to be monomeric [28] and will be referred to from now on as $NEMO_{355}$ (Figure 1). SEC-MALS allows the determination of an absolute molecular mass during analytical gel filtration, independent of the shape of the molecule under investigation, and hence is well suited to determine the oligomeric state of proteins. An initial MALS experiment reports a weight-averaged molecular mass (M_W) of 85.7 kDa for an average peak concentration of 1.4 μM, a value in close agreement with the formula molecular mass of dimeric $NEMO_{355}$ (83.8 kDa). However, at increased concentrations, elevated M_W values are apparent, a phenomenon that was unaffected when the NaCl concentration was increased to 500 mM (results not shown). We therefore analysed the concentration-dependent M_W of $NEMO_{355}$ further with a sequence of SEC-MALS analyses ranging from 1.4 to 16.9 μM (average peak concentration), as shown in Figure 2. These experiments reported corresponding M_W values of 85.7–113.8 kDa and clearly demonstrate that $NEMO_{355}$ is subject to concentration-dependent self-association based upon a minimum assembling unit equivalent to a dimer. The assembly of dimers into tetramers is the simplest model explaining these data.

In order to characterize further the size of the multimers involved in self-association, we investigated $NEMO_{355}$ using sedimentation velocity AUC at three concentrations: 8.8 μM, 17.6 μM, and 42 μM (monomer concentration). C(S) distribution analyses of the data clearly showed the presence of two major species centred at $s_{20,w}$ values of approx. 3 and 4 S (Figure 2). Consistent with the MALS data above, the relative peak proportions varied in a concentration-dependent manner. At low

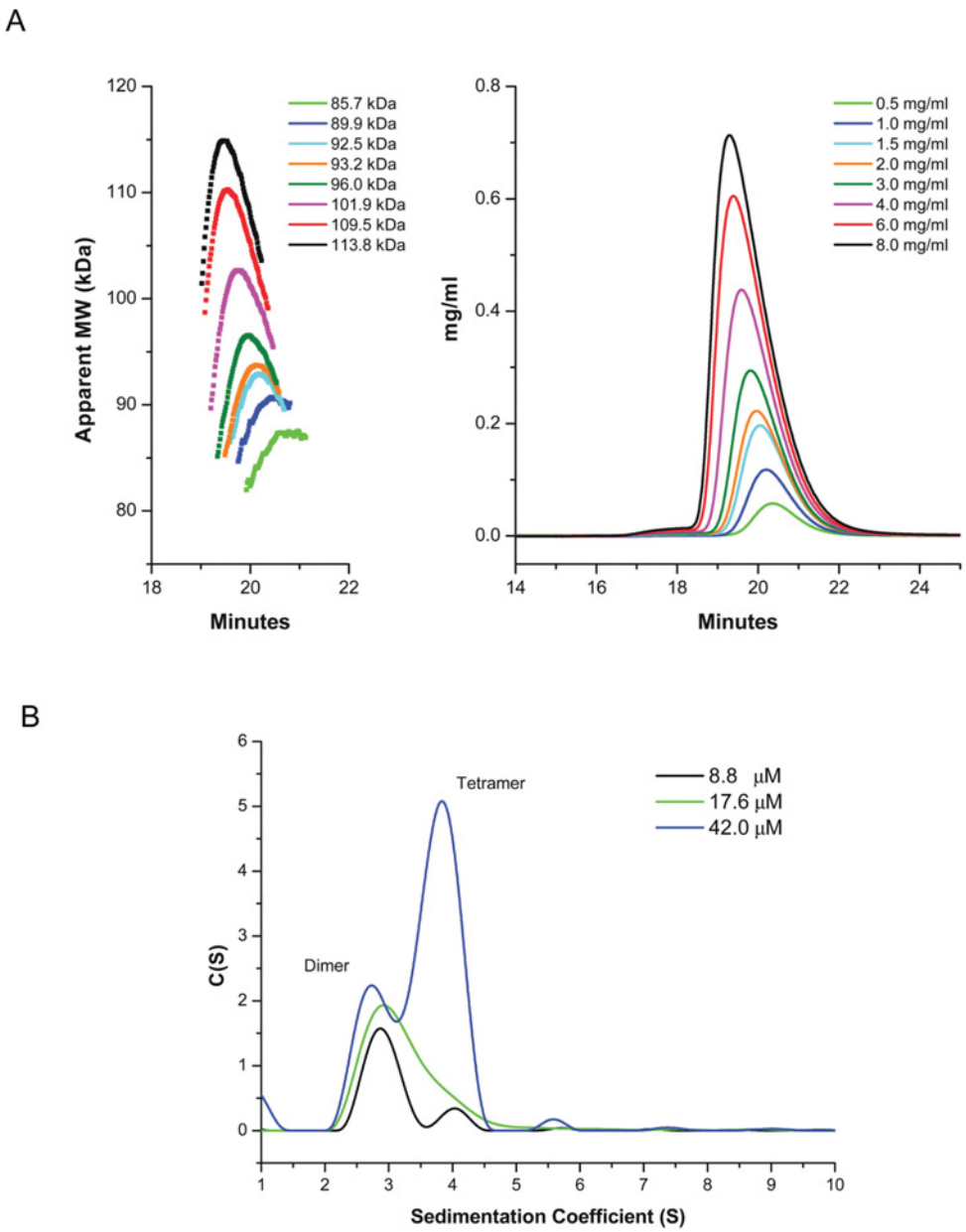

Figure 2 $NEMO_{355}$ is dimeric and exists in a concentration-dependent equilibrium with a higher order species

(**A**) SEC-MALS measurements of $NEMO_{355}$ (dimeric formula M_r 83.8 kDa) loaded at concentrations ranging from 0.5 to 8.0 mg/ml. Refractive index-derived weight concentrations (mg/ml) of the peaks are shown to the right. For clarity, derived M_w (kDa) of the peaks are shown separately to the left along with a legend detailing the peak M_w for each experiment. (**B**) $NEMO_{355}$ exists in a dimer/tetramer equilibrium. Sedimentation velocity experiments of $NEMO_{355}$ at three concentrations (8.8, 17.6 and 42 μM) shown as best-fit c(s) functions.

concentration, the predominant peak was centered on the lower $s_{20,w}$ value, whereas the reverse was true at higher concentration. At intermediate concentration (17.6 μM), the peaks were nearly indistinguishable. As the peaks were fully separated in the $c(s)$ function for the low-concentration experiment, we were able to analyse these data as discrete species. The data fitted well to a two-component discrete species model with $s_{20,w}$ values of 3.00 and 4.23 and $D_{t,20,w}$ (translational diffusion coefficient) values of 3.48 and 2.30 respectively (Figure 2 and Table 1). The respective M_W values calculated from these values are 77.6 and 164.9 kDa. These values are in good agreement with the molecular mass expected from $NEMO_{355}$ dimers (83.8 kDa) and tetramers (167.6 kDa). Using the relative peak proportions from the $c(s)$ function for the low concentration experiment (8.8 μM), an apparent dissociation constant (K_d) of 25.6 μM (dimer–tetramer equilibrium) was obtained. Notably, a fit of the SEC-MALS concentration-dependent data to a two-state self-association model resulted in an apparent K_d of 27.5 μM (results not shown).

In order to help identify the region responsible for NEMO tetramerization, isolated NEMO CoZi domain was also subjected to sedimentation-velocity analysis at 46, 93 and 139 μM monomer concentration (results not shown). The data from this experiment fitted well to a discrete species model showing a single significant component and M_w with a range of 25.0–27.8 kDa, consistent with the formula molecular mass of dimeric CoZi domain (25.9 kDa) (see Table 3). These results do not indicate the presence of the tetramers evident in the $NEMO_{355}$

Table 1 Hydrodynamic parameters of the 8.8 μM NEMO$_{355}$ sedimentation velocity experiment (discrete species model)

M_r, formula molecular mass; V_{bar}, partial specific volume; M_w, reported by experiment; $s_{20,w}$, sedimentation coefficient; $D_{t,20,w}$, translational diffusion coefficient; f/f_0, frictional coefficient ratio; K_d, dissociation constant, calculated from known loading concentration and relative peak proportions for a dimer–tetramer equilibrium; RMSD, average root mean square deviation of the fit. Parameters with only one value are independent of the particular species involved.

Parameters	Dimer	Tetramer
M_r (kDa)	83.8	167.6
V_{bar}	0.728	0.728
M_w (kDa)	77.6	164.9
$s_{20,w}$	3.00	4.23
$D_{t,20,w}$	3.5	2.3
f/f_0	2.3	2.6
Relative proportions	0.87	0.13
K_d (μM)	25.6	25.6
RMSD	0.057	0.057

construct, suggesting that the N-terminal region of NEMO is responsible for higher-order self-association.

NEMO adopts a highly elongated conformation

Importantly, the discrete species analysis of the AUC data also allowed us to calculate the frictional ratio (f/f_0) for CoZi and the NEMO$_{355}$ dimer and tetramer. The frictional ratio is a measure of the degree of asymmetry in a molecule with respect to an anhydrous sphere of the same mass. For CoZi, an f/f_0 of 1.7 was measured, which deviates considerably from the value (1.0) characteristic of a spherical protein molecule and points towards a highly elongated structure. Remarkably, the frictional ratios for NEMO$_{355}$ dimers and tetramers were significantly higher, 2.3 and 2.6 respectively, demonstrating that both are unusually elongated and asymmetric molecules in solution (Table 1).

IKK binding abolishes NEMO$_{355}$ tetramerization

The most highly recognized function of NEMO within the NF-κB signalling pathway is in the recruitment and regulation of IKKs responsible for the phosphorylation and inactivation of IκB. In order to further investigate the nature of the NEMO/IKK interaction, we analysed a complex of NEMO$_{355}$ and a 41-mer peptide comprising the IKKβ NEMO-binding domain (IKK$_{NBD}$; 4.7 kDa) by SEC-MALS analysis. The resulting M_w of the complex (92 kDa) was in close agreement with the formula molecular mass expected of dimeric NEMO$_{355}$ bound to two IKK$_{NBD}$ peptides (93.3 kDa) (Figure 3). This result agrees with a recently published heterotetrameric crystal structure comprising a short, dimeric NEMO N-terminal fragment bound to two IKK peptides [29]. Interestingly, the M_w reported by SEC-MALS remained constant over a wide NEMO$_{355}$ concentration range, demonstrating that the interaction is tight in accordance with previous studies [20,29]. Moreover, it shows that binding of IKK$_{NBD}$ completely abrogates the concentration-dependent tetramerization of NEMO$_{355}$. These results indicate that the IKK binding and tetramerisation regions are overlapping. Importantly, these data demonstrate that the oligomeric state of NEMO is modulated by binding of specific ligands.

The CoZi/di-ubiquitin interaction

Most ubiquitin-binding domains characterized so far interact with mono-ubiquitin, often with relatively low affinities [30,31].

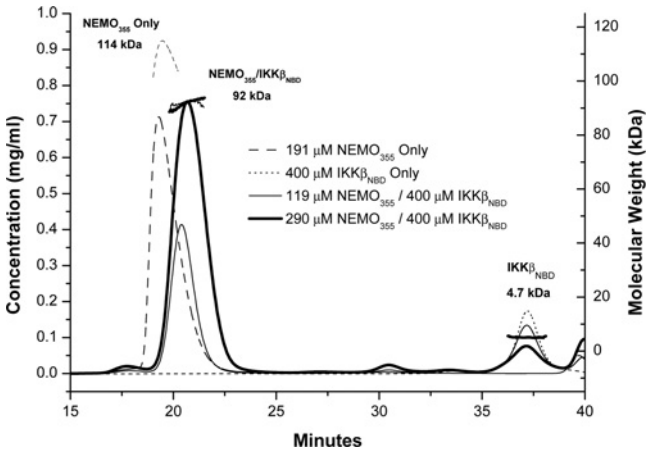

Figure 3 IKKβ C-terminal peptide tightly binds NEMO$_{355}$ and abrogates tetramerization

SEC-MALS measurements of high concentration NEMO$_{355}$ (dimeric formula M_r 83.8 kDa) bound to excess 41-mer C-terminal IKKβ peptide (4.7 kDa). RI-derived weight concentrations (mg/ml, left axis) of the peaks are shown for the entier run. In corresponding line types, derived apparent molecular mass (kDa, right axis) are shown for the centre of each peak. Shown for comparison is a measurement of a comparable concentration of NEMO$_{355}$ alone demonstrating an increase in M_w caused by tetramerization. Apparent molecular mass for the binding experiments ($\sim$92 kDa) agree with the formula molecular mass of dimeric NEMO$_{355}$ bound to two IKK peptides (93.3 kDa).

NEMO also binds very weakly to mono-ubiquitin [19] and surprisingly, only weakly to K63-linked di-ubiquitin, whereas the interaction with linear di-ubiquitin is around 100-fold stronger [17,18,26]. In order to understand better the thermodynamics of the interaction with linear ubiquitin chains, we used ITC to follow complex formation. No binding was detected between the CoZi domain and mono-ubiquitin at three different temperatures at concentrations of 50 μM CoZi in the cell and 500 μM ubiquitin in the syringe, indicating that any interaction must be very weak (results not shown). Titration of CoZi with increasing concentrations of di-ubiquitin at 18 °C resulted in heats of interaction that were too small for quantitative analysis. However, titrations at 25 °C and 10 °C produced sufficient signal to be able to fit the binding isotherm, resulting in dissociation constants of 1.4 and 2.6 μM respectively (see Table 2 and Figure 4A). Surprisingly, the stoichiometry of complex formation was $\sim$0.5 in terms of polypeptide chains, demonstrating that one CoZi dimer interacts with one molecule of di-ubiquitin. Given the pseudo-symmetrical structure of dimeric CoZi [17,18], one might expect that equivalent binding sites on each NEMO chain exist, and hence that two molecules of di-ubiquitin would bind, one either side (CoZi$_{dimer}$/2 $\times$ di-ubiquitin). In contrast, these binding studies suggest that the di-ubiquitin molecule interacts with NEMO in an asymmetric fashion. To test if this binding mode is preserved in the context of full-length NEMO, we titrated NEMO$_{355}$ with di-ubiquitin. As observed with the isolated CoZi domain, the enthalpy of complex formation was strongly temperature-dependent and endothermic at lower temperatures, but exothermic at room temperature (25 °C) and above. Notably, the binding stoichiometry and strength of complex formation are similar to that found for the CoZi domain with K_d values of 0.95 μM and 3.45 μM at 25 °C and 10 °C respectively (Table 2 and Figure 4B). However, there is some difference in the heat capacity change of complex formation, which is -587 cal $\cdot$ mol^{-1} $\cdot$ K^{-1} (1 cal $\approx$ 4.184 J) for CoZi and -360 cal $\cdot$ mol^{-1} $\cdot$ K^{-1} for the NEMO$_{355}$ di-ubiquitin interaction (Figure 4C).

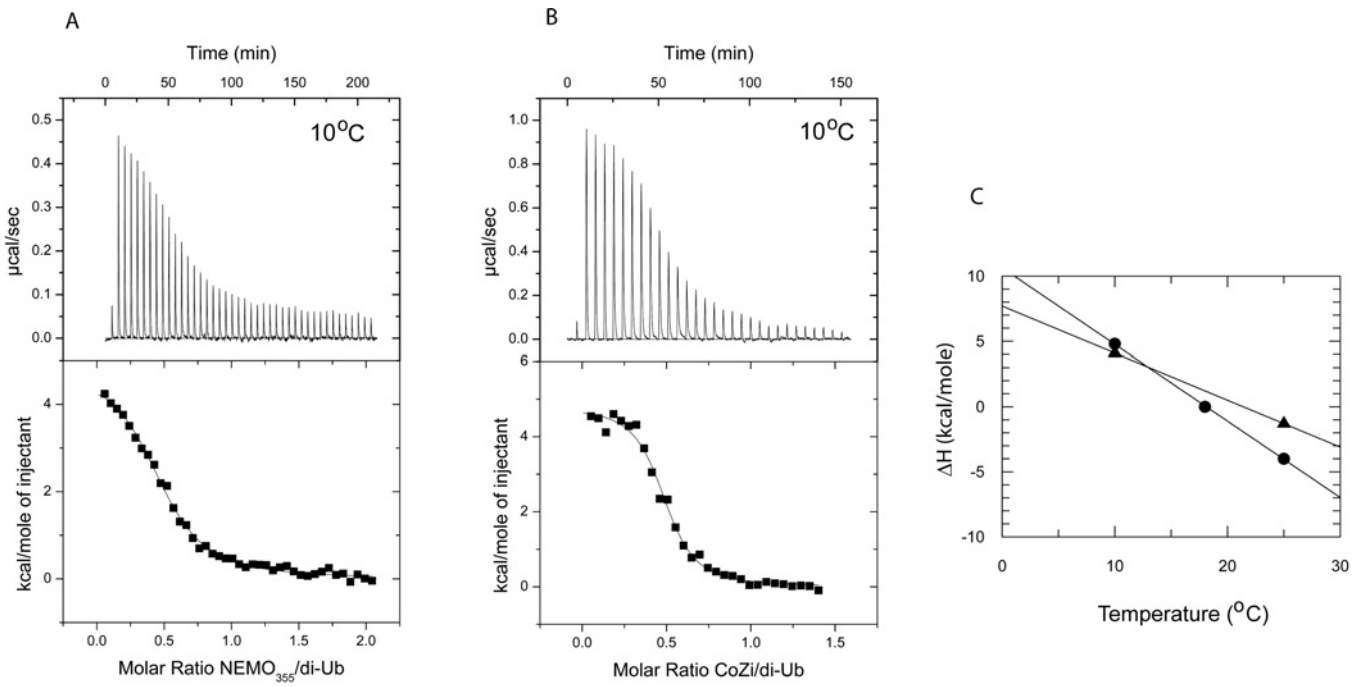

Figure 4 NEMO complexes with di-ubiquitin

ITC titrations of (**A**) 49.5 μM $NEMO_{355}$ titrated with 453 μM di-ubiquitin and (**B**) 112 μM CoZi titrated with 693 μM di-ubiquitin, both at 10 °C. (**C**) Enthalpies of complex formation are plotted as a function of temperature. The change in heat capacity is the slope of a linear regression fit.

Table 2 Thermodynamic parameters for the NEMO–di-ubiquitin interaction

All titrations were carried out three or four times and the estimated error is the S.D. between measurements.

Component in cell	T	N	K_d (μM)	ΔH (kcal/mol)
Mouse CoZi	10 °C	0.53 ± 0.06	2.6 ± 0.4	4.8 ± 0.6
	25 °C	0.62 ± 0.07	1.4 ± 1.0	−4.0 ± 0.6
Mouse $NEMO_{355}$	10 °C	0.44 ± 0.05	3.45 ± 0.4	4.1 ± 0.7
	25 °C	0.52 ± 0.04	0.95 ± 0.2	−1.3 ± 0.5

Analysis of NEMO–ubiquitin interaction by AUC

To investigate further the composition of the CoZi–di-ubiquitin complex and confirm the stoichiometry suggested by our ITC experiments, we characterized the CoZi–di-ubiquitin interaction by sedimentation-velocity AUC, which allows direct observation of the complex(es) under investigation. Multiple experiments were performed in which molar ratios of CoZi dimer and di-ubiquitin were varied (1:1, 1:2, 1:4 and 1:8; $CoZi_{dimer}$/di-ubiquitin). Molar concentrations and the resulting hydrodynamic data from these experiments are detailed in Table 3. In each of the three experiments where di-ubiquitin was present in stoichiometric excess, two discrete species were observed. The smallest component in each experiment clearly represents free di-ubiquitin, as the $s_{20,w}$ $D_{t,20,w}$ and M_W values closely correspond to the values obtained from analysis of di-ubiquitin alone (Table 3). In the 1:1 experiment, the largest and most abundant component has a mass of 45.3 kDa, close to the predicted molecular mass of a complex consisting of dimeric CoZi bound to one di-ubiquitin chain ($CoZi_{dimer}$–di-ubiquitin = 43.5 kDa). As expected, increasing the excess of di-ubiquitin resulted in increasing proportions of free di-ubiquitin. Unexpectedly,

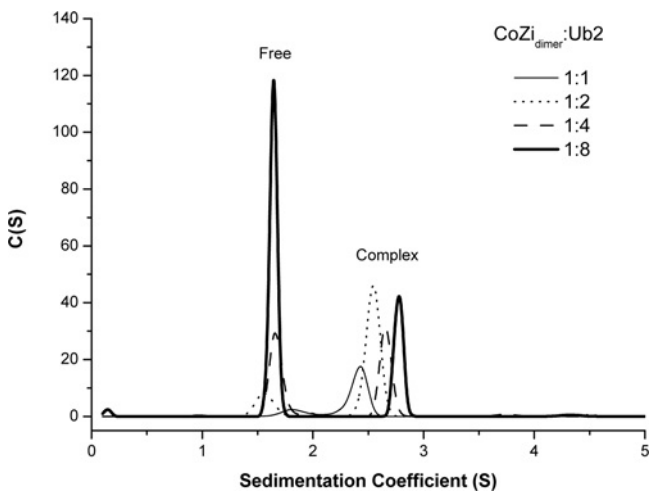

Figure 5 CoZi and di-ubiquitin interact to form $CoZi_{dimer}$/di-ubiquitin and at higher ubiquitin ratios $CoZi_{dimer}$/$(di\text{-}ubiquitin)_2$

Best fit C(S) functions for sedimentation velocity analysis of CoZi/di-ubiquitin (Ub2) interaction(s).

however, the apparent molecular mass of the complex component also increased with increasing excess of di-ubiquitin (Figure 5 and Table 3). At the highest ratio (1:8 $CoZi_{dimer}$/di-ubiquitin), the apparent mass increased to 53.3 kDa. This trend suggests formation of a complex containing a second di-ubiquitin bound to dimeric CoZi. We used the weight-averaged molecular mass (53.3 kDa) for the 1:8 experiment to determine the proportions of $CoZi_{dimer}$/di-ubiquitin and $CoZi_{dimer}$/$(di\text{-}ubiquitin)_2$, from which we can estimate a 100-fold weaker binding constant for the second di-ubiquitin binding site.

Table 3 Hydrodynamic parameters of the CoZi/di-ubiquitin interaction(s)

The first three columns denote the composition, reduced ratio, and molar ratios respectively at which the sedimentation-velocity experiments were carried out. All parameters are derived from discrete species modelling. Formula molecular mass: $CoZi_{dimer}$, 25.9 kDa; di-ubiquitin, 17.5 kDa; $CoZi_{dimer}$–di-ubiquitin, 43.5 kDa; $CoZi_{dimer}$–$(di\text{-}ubiquitin)_2$, 61.0 kDa. Partial specific volumes (V_{bar}): CoZi, 0.737; di-ubiquitin, 0.746; and averaged V_{bar} was used for CoZi–di-ubiquitin complexes. M_w, reported by experiment; $s_{20,w}$, sedimentation coefficient; $D_{t,20,w}$, translational diffusion coefficient; f/f_0, frictional ratio; RMSD, average root mean square deviation of the fit. Data are organized into sections pertaining either to free (unbound) or complex species and the nature of the free species is noted as $CoZi_{dimer}$, di-ubiquitin or Mixture (a weight-averaged mixture of unbound species).

		Concn.	Free					Complex				
	Ratio	(μM)	Free species	$s_{20,w}$	$D_{t,20,w}$	f/f_0	M_w	$s_{20,w}$	$D_{t,20,w}$	f/f_0	M_w	RMSD
$COZI_{dimer}$	–	23	$COZI_{dimer}$	1.76	6.5	1.7	25.0	–	–	–	–	0.0042
Di-ubiquitin	–	103	Di-ubiquitin	1.69	9.0	1.4	18.0	–	–	–	–	0.0063
$COZI_{dimer}$/di-ubiquitin	1:1	25:25	Mixture	2.08	9.3	1.6	20.9	2.55	5.3	1.7	45.3	0.0077
$COZI_{dimer}$/di-ubiquitin	1:2	45:90	Di-ubiquitin	1.76	9.1	1.3	17.9	2.67	5.7	1.6	43.7	0.0180
$COZI_{dimer}$/di-ubiquitin	1:4	25:100	Di-ubiquitin	1.71	9.0	1.3	17.9	2.76	5.7	1.5	45.9	0.0180
$COZI_{dimer}$/di-ubiquitin	1:8	25:200	Di-ubiquitin	1.71	9.7	1.3	16.6	2.89	5.1	1.5	53.3	0.0160

DISCUSSION

NEMO is the key regulatory component of the IKK complex that senses upstream stimulatory events and relays them to the activation of IKKα and IKKβ. A large proportion of the protein is predicted to form coiled coils, including the regions that are involved in ubiquitin recognition and interaction with the catalytic IKK subunits. The molecular mechanism by which NEMO induces activation of IKKα and IKKβ remains largely unknown, although various models have been suggested. One model assumes the CoZi domain undergoes stimulus-dependent conformational changes that in turn might induce activation of the kinases [19]. Alternatively, NEMO might act as a carrier or platform that is responsible for bringing IKKα and IKKβ in close proximity to activators such as TAK1 [TGFβ (transforming growth factor β)-activated kinase-1] to promote phosphorylation and activation ([23], but see [23a], [24]). On the other hand, the interaction with ubiquitin chains may induce clustering of NEMO, which could lead to IKK activation, possibly by inducing trans-phosphorylation.

In the present study we have characterized the oligomeric state of NEMO and its interaction with di-ubiquitin in order to provide a molecular basis for a better understanding of its role in NF-κB activation.

The oligomeric state of NEMO

The oligomeric state of NEMO has been controversial, and a number of different models have been suggested for the quaternary structure of the full-length protein as well as various fragments. Using a combination of MALS and AUC, we show that NEMO forms a very tight dimer that exists in a relatively weak equilibrium ($\sim$27 μM) with tetramers. Importantly, our extensive analysis shows that the protein preparations used in our study are homogeneous and monodisperse, and that no aggregates are present that may interfere with the measurements. Our results partially agree with a previous study that described human NEMO to predominantly form tetramers [15], but contradict a number of others that described NEMO as monomers and trimers [13,14,16]. The most likely explanation for this discrepancy is the presence of detergent in the work by Agou and co-workers, which was, apparently, required to prevent the formation of aggregates, suggesting that the protein used in those studies may not have been in its native conformation [13,14,16]. This interpretation is supported by the presence of chaperone protein DnaK in the protein preparations used for some of the studies. Furthermore, we believe that the various and highly contradicting oligomeric states determined for different N-terminal constructs of NEMO [20,21] are due to an inherent instability and heterogeneity of shorter NEMO fragments, which may have compromised previous work. This interpretation is supported by Rushe et al. [29] who reported a similar lack of homogeneity for shorter N-terminal fragments of NEMO.

In contrast with $NEMO_{355}$, the CoZi domain has no tendency to tetramerize over a range of concentrations. Furthermore, complex formation with an IKKβ-derived peptide completely abolished the ability of dimeric $NEMO_{355}$ to form higher-order oligomers, showing that the region surrounding the IKK-binding site is responsible for tetramerization. These results from the present study are in contrast with those of previous cross-linking studies, which suggested that NEMO binds the IKKs in its tetrameric form and that tetramerization is required for kinase activity [15]. It now seems likely that cross-linking studies have overestimated the oligomeric state of NEMO due to non-specific association. Nevertheless, the model that oligomerization of NEMO might be part of the IKK activation mechanism is intriguing and is fully compatible with the notion that binding to polyubiquitin chains induces clustering of NEMO as described below. Importantly, the observation that interaction with IKK abolishes tetramerization clearly illustrates that the oligomeric state of NEMO in its ligand complexes might differ from that of the apoprotein.

Similarly to full-length NEMO, the state of the minimal oligomerization domain, CoZi, has been controversial. Two recent crystal structures of the apo form of this domain show it to form a parallel coiled-coil domain that is approx. 120 Å (1 Å = 0.1 nm) in length [17,18]. This is in accordance with the results reported here, yet contradicts a number of other studies that reported trimeric and hexameric assemblies [13,16]. A CoZi construct comprising amino acids 250–339 has been reported to exist in a monomer–dimer equilibrium with a K_d of 30 μM [19]. The fragment used in the present study is slightly extended at the C-terminus and includes amino acids 340–355, which are not predicted to be part of the LZ. Interestingly, the inclusion of this region significantly strengthens dimerization, suggesting that this C-terminal extension, which is absent in the crystallised fragments, is part of the coiled-coil domain.

AUC studies of $NEMO_{355}$ show that it adopts an extremely elongated conformation, as illustrated by the frictional ratios for $NEMO_{355}$ dimers and tetramers (2.3 and 2.6 respectively). These values are significantly higher than would be expected for a globular protein and are in fact similar to the value measured for fibrinogen (2.3), a rod-like protein that has been shown by electron microscopy to have an average axial ratio (length divided by diameter) of 7.5 [32–34]. The recently reported

structures of $NEMO_{44-111}$ bound to IKK-derived peptides [29] and $NEMO_{150-272}$ bound to vFLIP [35] show the respective ligand-bound fragments of NEMO form an elongated dimeric coiled-coil. In combination with our AUC studies, these observations indicate that binding of target proteins will not induce gross conformational changes, but can alter oligomerization. Instead, apo-NEMO forms a highly elongated coiled-coil that is poised to accommodate the binding of different proteins, apparently without major structural rearrangements. Nevertheless, it is tempting to speculate that binding to ligands may induce slight local changes that are propagated along the coiled-coil, ultimately inducing activation of IKKα and IKKβ.

The NEMO–polyubiquitin interaction

The interaction of NEMO with polyubiquitin chains is important for the activation of the IKK complex in response to TNFα stimulation ([23], but see [23a], [24]). Binding occurs via the UBAN motif within the CoZi domain. The interaction of mono-ubiquitin with CoZi is extremely weak, and we could not detect any binding under the conditions of our ITC experiments, although high sensitivity LUMIER (LUminescence-based Mammalian IntERactome) assays showed weak binding can occur [19]. In contrast, linear di-ubiquitin binds with an affinity in the low-micromolar range, clearly indicating that the interaction with each individual ubiquitin is additive. Unexpectedly, binding of NEMO to K63-linked di-ubiquitin is significantly weaker than to linear chains [17,18,26], suggesting that linear polyubiquitin chains may be the true physiological targets [18].

The stoichiometry of the CoZi–di-ubiquitin interaction determined in our ITC experiments indicated that one NEMO dimer interacts with one molecule of di-ubiquitin. This stoichiometry is in accordance with an independent study by Lo et al. [17] that also detected a 2:1 complex in solution. On the basis of NMR chemical shift perturbations and mutagenesis studies, these authors suggested a model for the complex in which di-ubiquitin clasps around dimeric NEMO roughly perpendicular to the long axis of the NEMO coiled-coil domain. However, this stoichiometry and the derived model strongly contradict the recently published CoZi/di-ubiquitin structure, which instead shows two molecules of di-ubiquitin to bind to a NEMO dimer in an orientation that is parallel with the coiled-coil axis [18]. Moreover, the authors of this study present NF-κB activation assays with NEMO mutants defective in ubiquitin binding, which support the notion that binding of two di-ubiquitin molecules to NEMO is physiologically important. A simple explanation for the apparent discrepancy between these studies could be the partial dissociation of CoZi in the solution studies. However, this explanation seems highly unlikely, as our AUC sedimentation analysis of CoZi at concentrations used in the ITC experiments shows that CoZi exists entirely in its dimeric form.

Interestingly, in solution $NEMO_{355}$ shows similar binding properties towards di-ubiquitin in terms of stoichiometry and apparent affinity as the CoZi domain, whereas the thermodynamic characteristics of complex formation show small but distinctive differences. This observation implies that binding of ubiquitin does not induce any large conformational changes in the region N-terminal to the CoZi domain, since this would probably be reflected in the affinity of the interaction. Nevertheless, it indicates that some communication exists between the CoZi domain and the N-terminal part of NEMO.

To gain further insight into the CoZi–di-ubiquitin interaction and understand the apparently conflicting binding stoichiometries, we analysed complexes at different NEMO/di-ubiquitin ratios by AUC. Sedimentation velocity experiments, at equimolar concentrations of CoZi dimers and di-ubiquitin, showed a complex of the molecular mass expected from the stoichiometry observed in our ITC studies. Intriguingly, however, increases in the relative ratio of di-ubiquitin over CoZi led to an increase in the apparent molecular mass of the complex, suggesting that at higher concentrations of di-ubiquitin a second binding site in NEMO becomes occupied. Affinity for this second site is significantly weaker, and thus it is possible that binding of the first molecule of di-ubiquitin may occlude binding of a second. However, high ubiquitin concentrations might induce slight structural rearrangements in NEMO, which in turn allow the second binding site to become accessible. Alternatively, apo-NEMO might exist in an equilibrium between two states, of which only one may be capable of binding two di-ubiquitin chains. This state might be unfavourable and hence would only be occupied at high ubiquitin concentrations. However, crystallization conditions might have selected for this state over the other.

It is tempting to speculate that, *in vivo*, a multi-protein complex containing ubiquitinated proteins such as RIP1 may provide the high ubiquitin density required for occupation of the second site. Population of the second site might be the trigger to initiate IKK activation, possibly through clustering of NEMO. In fact, this two-site binding event might constitute a 'threshold for activation' to prevent non-specific activation of NF-κB, which can have detrimental consequences for the host. Further studies are now required to better characterize the *in vivo* role of these two binding sites and understand the molecular events leading to their formation.

AUTHOR CONTRIBUTION

Frank Ivins designed and performed experiments, analysed data and wrote the manuscript; Mark Montgomery designed and performed experiments and analysed data; Susan Smith and Aylin Morris-Davies performed experiments; Ian Taylor designed experiments and analysed data; and Katrin Rittinger designed the study, analysed data and wrote the manuscript.

ACKNOWLEDGEMENTS

We thank Steve Smerdon [NIMR (National Institute for Medical Research)], Felix Randow [MRC-LMB (Medical Research Council-Laboratory of Molecular Biology)] and Ben Stieglitz (NIMR) for helpful discussions and critical reading of the manuscript before its submission.

FUNDING

This work was supported by the Medical Research Council, U.K.

REFERENCES

1 Hayden, M. S. and Ghosh, S. (2008) Shared principles in NF-κB signaling. Cell **132**, 344–362
2 Ghosh, S. and Karin, M. (2002) Missing pieces in the NF-κB puzzle. Cell **109**, S81–S96
3 Rothwarf, D. M., Zandi, E., Natoli, G. and Karin, M. (1998) IKK-γ is an essential regulatory subunit of the IκB kinase complex. Nature **395**, 297–300
4 Yamaoka, S., Courtois, G., Bessia, C., Whiteside, S. T., Weil, R., Agou, F., Kirk, H. E., Kay, R. J. and Israel, A. (1998) Complementation cloning of NEMO, a component of the IκB kinase complex essential for NF-κB activation. Cell **93**, 1231–1240
5 Scheidereit, C. (2006) IκB kinase complexes: gateways to NF-κB activation and transcription. Oncogene **25**, 6685–6705
6 DiDonato, J. A., Hayakawa, M., Rothwarf, D. M., Zandi, E. and Karin, M. (1997) A cytokine-responsive IκB kinase that activates the transcription factor NF-κB. Nature **388**, 548–554
7 Mercurio, F., Zhu, H., Murray, B. W., Shevchenko, A., Bennett, B. L., Li, J., Young, D. B., Barbosa, M., Mann, M., Manning, A. and Rao, A. (1997) IKK-1 and IKK-2: cytokine-activated IκB kinases essential for NF-κB activation. Science **278**, 860–866
8 Regnier, C. H., Song, H. Y., Gao, X., Goeddel, D. V., Cao, Z. and Rothe, M. (1997) Identification and characterization of an IκB kinase. Cell **90**, 373–383
9 Poyet, J. L., Srinivasula, S. M., Lin, J. H., Fernandes-Alnemri, T., Yamaoka, S., Tsichlis, P. N. and Alnemri, E. S. (2000) Activation of the IκB kinases by RIP via IKKγ/NEMO-mediated oligomerization. J. Biol. Chem. **275**, 37966–37977

10 Sebban, H., Yamaoka, S. and Courtois, G. (2006) Posttranslational modifications of NEMO and its partners in NF-κB signaling. Trends Cell. Biol. **16**, 569–577
11 Sun, S. C. and Yamaoka, S. (2005) Activation of NF-κB by HTLV-I and implications for cell transformation. Oncogene **24**, 5952–5964
12 Field, N., Low, W., Daniels, M., Howell, S., Daviet, L., Boshoff, C. and Collins, M. (2003) KSHV vFLIP binds to IKK-γ to activate IKK. J. Cell. Sci. **116**, 3721–3728
13 Agou, F., Ye, F., Goffinont, S., Courtois, G., Yamaoka, S., Israel, A. and Veron, M. (2002) NEMO trimerizes through its coiled-coil C-terminal domain. J. Biol. Chem. **277**, 17464–17475
14 Fontan, E., Traincard, F., Levy, S. G., Yamaoka, S., Veron, M. and Agou, F. (2007) NEMO oligomerization in the dynamic assembly of the IκB kinase core complex. FEBS J. **274**, 2540–2551
15 Tegethoff, S., Behlke, J. and Scheidereit, C. (2003) Tetrameric oligomerization of IκB kinase γ (IKKγ) is obligatory for IKK complex activity and NF-κB activation. Mol. Cell. Biol. **23**, 2029–2041
16 Agou, F., Traincard, F., Vinolo, E., Courtois, G., Yamaoka, S., Israel, A. and Veron, M. (2004) The trimerization domain of NEMO is composed of the interacting C-terminal CC2 and LZ coiled-coil subdomains. J. Biol. Chem. **279**, 27861–27869
17 Lo, Y. C., Lin, S. C., Rospigliosi, C. C., Conze, D. B., Wu, C. J., Ashwell, J. D., Eliezer, D. and Wu, H. (2009) Structural basis for recognition of diubiquitins by NEMO. Mol. Cell **33**, 602–615
18 Rahighi, S., Ikeda, F., Kawasaki, M., Akutsu, M., Suzuki, N., Kato, R., Kensche, T., Uejima, T., Bloor, S., Komander, D. et al. (2009) Specific recognition of linear ubiquitin chains by NEMO is important for NF-κB activation. Cell **136**, 1098–1109
19 Bloor, S., Ryzhakov, G., Wagner, S., Butler, P. J., Smith, D. L., Krumbach, R., Dikic, I. and Randow, F. (2008) Signal processing by its coil zipper domain activates IKKγ. Proc. Natl. Acad. Sci. U.S.A. **105**, 1279–1284
20 Drew, D., Shimada, E., Huynh, K., Bergqvist, S., Talwar, R., Karin, M. and Ghosh, G. (2007) Inhibitor κB kinase β binding by inhibitor κB kinase γ. Biochemistry **46**, 12482–12490
21 Lo, Y. C., Maddineni, U., Chung, J. Y., Rich, R. L., Myszka, D. G. and Wu, H. (2008) High-affinity interaction between IKKβ and NEMO. Biochemistry **47**, 3109–3116
22 Marienfeld, R. B., Palkowitsch, L. and Ghosh, S. (2006) Dimerization of the IκB kinase-binding domain of NEMO is required for tumor necrosis factor α-induced NF-κB activity. Mol. Cell. Biol. **26**, 9209–9219
23 Wu, C. J., Conze, D. B., Li, T., Srinivasula, S. M. and Ashwell, J. D. (2006) Sensing of Lys 63-linked polyubiquitination by NEMO is a key event in NF-κB activation. Nat. Cell Biol. **8**, 398–406
23a Erratum (2006) Nat. Cell Biol. **8**, 424
24 Ea, C. K., Deng, L., Xia, Z. P., Pineda, G. and Chen, Z. J. (2006) Activation of IKK by TNFα requires site-specific ubiquitination of RIP1 and polyubiquitin binding by NEMO. Mol. Cell **22**, 245–257
25 Wagner, S., Carpentier, I., Rogov, V., Kreike, M., Ikeda, F., Lohr, F., Wu, C. J., Ashwell, J. D., Dotsch, V., Dikic, I. and Beyaert, R. (2008) Ubiquitin binding mediates the NF-κB inhibitory potential of ABIN proteins. Oncogene **27**, 3739–3745
26 Komander, D., Reyes-Turcu, F., Licchesi, J. D., Odenwaelder, P., Wilkinson, K. D. and Barford, D. (2009) Molecular discrimination of structurally equivalent Lys 63-linked and linear polyubiquitin chains. EMBO Rep. **10**, 466–473
27 Tokunaga, F., Sakata, S. I., Saeki, Y., Satomi, Y., Kirisako, T., Kamei, K., Nakagawa, T., Kato, M., Murata, S., Yamaoka, S. et al. (2009) Involvement of linear polyubiquitylation of NEMO in NF-κB activation. Nat. Cell Biol. **11**, 123–132
28 Cordier, F., Vinolo, E., Veron, M., Delepierre, M. and Agou, F. (2008) Solution structure of NEMO zinc finger and impact of an anhidrotic ectodermal dysplasia with immunodeficiency-related point mutation. J. Mol. Biol. **377**, 1419–1432
29 Rushe, M., Silvian, L., Bixler, S., Chen, L. L., Cheung, A., Bowes, S., Cuervo, H., Berkowitz, S., Zheng, T., Guckian, K. et al. (2008) Structure of a NEMO/IKK-associating domain reveals architecture of the interaction site. Structure **16**, 798–808
30 Hurley, J. H., Lee, S. and Prag, G. (2006) Ubiquitin-binding domains. Biochem. J. **399**, 361–372
31 Hicke, L., Schubert, H. L. and Hill, C. P. (2005) Ubiquitin-binding domains. Nat. Rev. Mol. Cell Biol. **6**, 610–621
32 Hall, C. E. and Slayter, H. S. (1959) The fibrinogen molecule: its size, shape, and mode of polymerization. J. Biophys. Biochem. Cytol. **5**, 11–16
33 Weisel, J. W., Phillips, Jr, G. N. and Cohen, C. (1981) A model from electron microscopy for the molecular structure of fibrinogen and fibrin. Nature **289**, 263–267
34 Smith, M. H. (1970) Handbook of Biochemistry-Selected Data for Molecular Biology. CRC Press+, Cleveland
35 Bagneris, C., Ageichik, A. V., Cronin, N., Wallace, B., Collins, M., Boshoff, C., Waksman, G. and Barrett, T. (2008) Crystal structure of a vFlip-IKKγ complex: insights into viral activation of the IKK signalosome. Mol. Cell **30**, 620–631

Received 13 March 2009/1 May 2009; accepted 7 May 2009
Published as BJ Immediate Publication 7 May 2009, doi:10.1042/BJ20090427